Slow Neutron Velocity Spectrometer Studies. IV. Au, Ag, Br, Fe, Co, Ni, Zn

W. W. HAVENS, JR., AND L. J. RAINWATER
Columbia University, New York, New York
(Received May 23, 1951)

The spectrometer has been improved, enlarged, and all the operational factors re-evaluated. The principal resonance in gold has been redetermined as $E_0=4.87\pm0.07$ ev, and in silver as 5.13 ± 0.07 ev. Resonances are found in Br at 35.7, 54, 104, and 136 ev. Transmission dips are also observed at higher energies which are probably due to unresolved levels. The thermal cross section of iron is well matched by the relation $\sigma=(11.2+0.33E^{-\frac{1}{2}})$. Crystal interference effects are observed in the thermal region with the Debye-Scherrer rings at 2.3A and 2.8A resolved. The cut-off wavelength predicted to be at 4.04A is in good agreement with experiment. No strong resonances are observed in iron at high energies. Resonances are observed in cobalt at 126 ev and 5000 ev. Ni shows crystal interference effects in the thermal region. No strong resonances were detected at high energies. The thermal cross section of Zn is well matched by the relation $\sigma=3.85+0.14E^{-\frac{1}{2}}$ with crystal interferences effects observed in the thermal region. Resonances in Zn occur at 520 ev, 1100 ev, and 3800 ev.

A. INTRODUCTION

THE results of previous investigations using the Columbia University slow neutron velocity spectrometer have been presented in a number of earlier papers.[1-3] The previous three papers[2] of this series present the results of survey studies of nuclear resonance levels using a spectrometer system, which employs a 100-kc crystal oscillator as the timing standard and permits simultaneous measurement of 16 energy intervals for each of two counter systems. Some of the work which has been published[1,3] was not included in this series, as part of it referred to different types of investigations and part of it was done using the original spectrometer system which had considerably poorer reliability and resolving power.

B. IMPROVEMENT OF THE SPECTROMETER CIRCUITS

The spectrometer system described in the first paper of this series has been improved by replacing the 100-kc crystal oscillator with a 1-megacycle crystal oscillator. The block diagram for the spectrometer system is essentially the same as Fig. 1 of the first paper of this series,[2] except that the 100-kc oscillator and 5-μsec circuit are replaced by a 1-Mc oscillator and five additional timing scale-of-two circuits. This permits timing pulses of 1, 2, 4, 8$\cdots$, 32768 μsec. In practice detection intervals as short as 2 μsec and arc "on times" as low as 4 μsec were used for the highest resolution studies to give an approximately triangular resolution function of about 1 μsec/meter width at the base. A 6-meter path length was used for almost all of the measurements.

An arc "on time" of $\tau_{arc}=4$ μsec rather than 2 μsec is used for intensity reasons. The effective arc "on time" is not a square pulse of 4 microseconds duration because the arc current takes between $\frac{1}{2}$ and 1 μsec to rise to its full value. For very sharp dips there is some advantage in having points more closely spaced than the resolution width of the apparatus to better define the transmission curve. Thus it is better to keep the detection intervals (and spacing) shorter than the arc "on time" for highest resolution work.

In the course of the circuit revision, the speed of operation of the entire system was greatly improved in all parts including the pulse amplifiers, pulse-height selectors, timing coincidence circuits, and other timing circuits.

C. QUENCHING THE ARC PULSE

In normal operation of the spectrometer it was customary to remeasure a sharp resonance dip as a general check on the over-all operation of the system from time to time. Such checks made shortly after the publication of the previous set of papers[2] showed a smearing of the resonance dips of Co, Ag, and Au to give much broader and shallower dips displaced to larger timings, and with slow recovery of the transmission on the low energy side of the dip. This was interpreted as failure of the ion production at the arc to stop at the end of the arc modulation pulse. The magnitude of this effect remained large for a period of time and many attempts were made to locate the cause of the trouble and correct it. The cyclotron used a hooded capillary type arc source and the effect was probably caused by ions produced lower down in the arc source which were gradually blown out after the electron emission from the filament was ended. However, the operating conditions were, as far as was known, the same as for the earlier measurements which had shown no observable smearing effect. Thus, under apparently identical operating conditions, the system developed a bad gradual trailing off of ion production after the arc pulse was over. By keeping the flow of deuterium to the arc to a minimum the effect could be removed. The intensity was greatly reduced but the resonance dips

[1] L. J. Rainwater and W. W. Havens, Jr., Phys. Rev. **70**, 136 (1946); W. W. Havens, Jr., and L. J. Rainwater, Phys. Rev. **70**, 154 (1946).
[2] Rainwater, Havens, Wu, and Dunning, Phys. Rev. **71**, 65 (1947); Havens, Wu, Rainwater, and Meaker, Phys. Rev. **71**, 165 (1947); Wu, Rainwater, and Havens, Phys. Rev. **71**, 174 (1947).
[3] Rainwater, Havens, Dunning, and Wu, Phys. Rev. **73**, 733 (1948); Havens, Rainwater, Wu, and Dunning, Phys. Rev. **73**, 963 (1948).

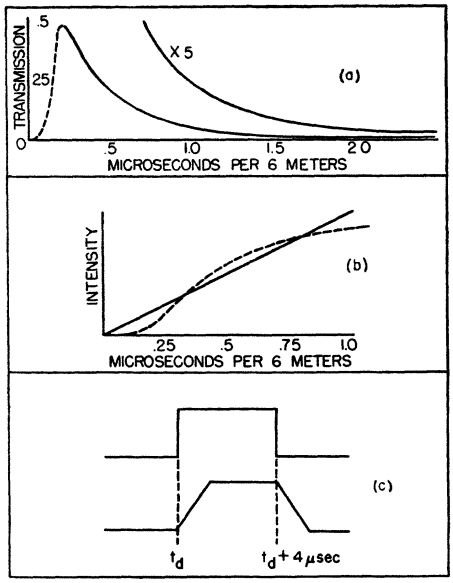

FIG. 1. Calibration of over-all delay time of apparatus. The solid curve in (a) shows the calculated transmission of the thick paraffin sample. The dashed part of the curve indicates the change in neutron intensity. The dashed curve in (b) shows the relative intensity near zero timing; the solid line is the straight line approximation used. The upper curve in (c) shows the theoretical neutron production; the lower curve the approximate neutron production used in the analysis of results.

were restored to the correct timings. The magnitude of the shifts, at worst, was such that the gold and silver resonances were moved from timing values corresponding to ~5 ev to values near 4 ev energy.

The solution which has finally been adopted is to separate the hood on the arc source from the grounded capillary tube and maintain it at a positive potential of about 2000 volts. This potential repels any positive ions in the capillary tube and prevents delayed emission from plasma blown out of the lower part of the arc source. A negative potential was found to make the effect worse and too small a positive voltage did not improve conditions since it could not overcome the effect of the gas flow sweeping the ions out of the capillary. In all measurements using moderately high resolution, the high quenching voltage is now used while the electrode is grounded for low resolution or unmodulated cyclotron operation. Thus, while the effect of delayed ion emission has been cured, the reason why there was no indication of such effects in the earlier work or why the effect suddenly became large is not understood. Such effects appear to be absent from the Cornell cyclotron velocity selector.[4]

D. CALIBRATION OF THE OVER-ALL DELAY TIME

The energy of a resonance dip is determined by the source-detector path length of 6 meters and by the time-of-flight of the neutrons of this energy. The timing of a detection interval after the arc modulation pulse is well known in terms of the basic timing circuits which are precise to ~0.1 μsec. There is, however, a certain over-all delay time, t_d, of the system representing the time required to accelerate the deuterons, etc., and this must be accurately evaluated. Measurements were previously made with the BF_3 counter in a B_4C shield near the source and showed a 7 μsec delay time using 2 μsec arc and detection intervals. Thus, for most of a the subsequent work a 7 μsec correction was used. However, this delay time varies slightly with operating conditions and therefore a technique has been devised to measure the delay time under the same operating conditions and during the same operating period in which the resonance dips are measured. The results of these checks now indicate that a value of between 8.5 and 10.0 μsec is usually obtained with the exact value varying over this range between successive operating periods. The shift from the original value to 9.0 μsec is 2.0 μsec in 6 meters or 0.32 μsec/meter. The position of resonances obtained using this correction now checks very closely the results of Selove *et al.*, using the Argonne mechanical velocity spectrometer system.[5] When the arc and detection intervals are not equal, there is an additional correction of half the difference in the widths if the timings are referred to the start of the intervals rather than to the centers. For $\tau_{arc}=4$ μsec and $\tau_{det}=2$ μsec, this increases the apparent value of t_d by 1 μsec.

The method which is now used to check the delay time is quite simple and consists of using the first detection group[2] and inserting a 2.89 g/cm² paraffin filter in the neutron beam. This gives calculated transmission values of 0.47, 0.237, 0.050, 0.022, 0.011, and 0.0043, at 4×10^6, 10^6, 2×10^5, 10^5, 5×10^4, and 10^4 ev respectively. Thus, only fast neutrons having time-of-flight values of less than 1 μsec for 6 meters will contribute significantly to the counting rate, and the counting rate *vs* timing interval almost gives the experimental resolution function with the delay time shift. In Fig. 1(a) the calculated transmission[6] is given as a function of neutron time-of-flight. If the arc pulse is turned on between $t=0$ and $t=4$ μsec from the start of the timing cycle, the delay time, t_d, will cause the effective neutron production "on time" to be displaced to between t_d and (t_d+4 μsec) as shown in the upper curves of Fig. 1(c).

If infinitely short detection intervals were used and there was zero source detector distance, then the plot of detected intensity *vs* timing for fast neutrons should also be zero outside of the region t_d to (t_d+4 μsec) and constant within. Again for infinitely narrow detection intervals but with the detector at 6 meters and using the thick paraffin filter, the plot will be broadened as shown in the second curve of Fig. 1(c). This curve may

[4] B. D. McDaniel, Phys. Rev. **70**, 832 (1946).

[5] W. Selove, Phys. Rev. **77**, 557 (1950). Hibdon, Muehlhause, and Selove, Phys. Rev. **77**, 730 (1950).

[6] R. K. Adair, Revs. Modern Phys. **22**, 249 (1950). H. J. Groenewald and H. Groendijk, Physica **XIII**, No. 1-3 (1947).

be understood by noting that the neutrons of a given timing must have originated at the source slab at a time earlier by the amount of the time-of-flight. Since neutrons with times-of-flight between ~0.2 and 1 μsec for 6 meters make up most of the neutrons detected, the expected counting rate will increase roughly linearly for t_d to $(t_d+1$ μsec) and then remain constant until $(t_d+4$ μsec) after which it falls off in another microsecond. Thus the expected intensity *vs* timing is not just the experimental resolution function displaced by t_d but is broadened by about 1 μsec extra and is shifted to larger timings by about 0.5 μsec (at 6 meters).

More precisely, to construct the lower curve of Fig. 1(c) the transmission curve of Fig. 1(a) should be multiplied by the curve giving the relative number of neutrons from the source per unit time-of-flight interval times the relative detection efficiency of the BF_3 counter. If the area of this resulting curve is normalized to unity, the integral of the curve should give the form of the rise and fall-off of the lower curve of Fig. 1(c). This is shown in Fig. 1(b) roughly, and a comparison straight line rise between zero and 1 μsec/6 meters is seen to give a good approximation. This approximation was used in Fig. 1(c) and in the analysis of the experimental intensity *vs* timing curve using the thick paraffin.

In Fig. 2, two curves are shown illustrating extreme variations of the measured curves at different operating periods. The procedure which has now been adopted is to check the position of energy levels by frequent measurements using the thick paraffin to determine t_d at the time of the measurements of the position of the resonance dip. The position of the dips for several elements which were previously investigated have been checked by this method, and the results are presented in this and later papers.

E. CALIBRATION OF THE EFFECTIVE SOURCE-DETECTOR DISTANCE

The energy of the neutron groups is determined by the time-of-flight over a measured path length. However, there is a small uncertainty in how this distance should be measured. At the detector end, the center of the 10 cm long active region of the BF_3 counter is used as the detector position while the finite length of the detector contributes an extra term to the resolution broadening, amounting to 1/60 of the time-of-flight. The position to be taken as the effective source location has the main uncertainty due to the small effect of the mean time required for neutrons to cascade from higher energies to the energy of the group being measured. This cascading time is inversely proportional to the velocity of the neutron group being studied, and thus it acts like an extra contribution to the source detector distance to be added to the distance from the front of the source to the detector.

To measure this effective increase in path length, a method of differences has been employed. Using a nominal source detector distance $l_1 \approx 1$ meter, the timing positions of the main resonances at t_{11} and t_{12} for cobalt and indium (126 ev and 1.45 ev) were determined. The same resonances were then studied at $l_2 \approx 6$ meters giving timings t_{21} and t_{22}. The differences $\Delta t_1=(t_{12}-t_{11})$ and $\Delta t_2=(t_{22}-t_{21})$ then give the differences in timing for the two resonances at l_1 and l_2. Now l_1 and l_2 can be measured quite precisely aside from the correction effect mentioned above, so the difference $l_2-l_1 \approx 5$ meters is known with considerable accuracy. The difference $(\Delta t_2-\Delta t_1)$ accurately corresponds to the timing difference of the two levels for a path length (l_2-l_1). The effective path l_1 is then given by

$$l_1(\text{effective})=(l_2-l_1)\Delta t_1/(\Delta t_2-\Delta t_1).$$

It should be noted that this method does not require a precise knowledge of the effective time delay or of the energies E_1 and E_2. Such measurements gave a 3 cm effective increase in the path length which is in good agreement with theory. Groenewald and Groendijk[6] [Eq. (23) of their paper] show that the average time a neutron emitted with energy $E \leq E_{\text{initial}}$ has been in paraffin is $\approx 3\tau(E)$. This corresponds to adding three times the mean free path (0.7 cm) for collisions at this energy or 2.1 cm. However, we measure to the part of the source slab which has a plywood front. The equivalent surface of paraffin is thus slightly less than one centimeter further away so that this adds up essentially to 3 cm.

As a by-product of this calibration, when combined with the measurement of the energy of the Co resonance described later, a new value of (1.45±0.02) ev is obtained for the indium resonance. This result is considered to be better established than the previous value[2] of (1.44±0.02) ev. The stated limits of error are now felt to represent extreme limits of uncertainty.

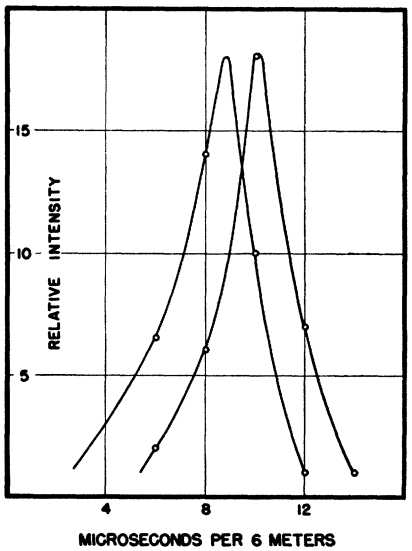

FIG. 2. These two curves show the extreme variations of the measured delay time at different operating periods.

F. ANALYSIS OF RESONANCE LEVEL PARAMETERS

The observation of the time-of-flight corresponding to the minimum of a sharp transmission dip determines the time-of-flight, t_0, and thus the energy, E_0, corresponding to exact resonance. If $n\sigma_0 \gg 1$ where n = sample thickness in atoms/cm^2 and σ_0 = total cross section at exact resonance, calculated for the natural element, the "strength" of the level $\sigma_0\Gamma^2$ can be determined from the area of the transmission dip as described in an earlier paper.[1] Here Γ is the full level width at half-maximum cross section. If $\Gamma \ll E_0$ so the "$(1/v)$ factor" can be neglected, the expression for the total cross section of an element near resonance (neglecting doppler broadening) can be given as

$$\sigma = \sigma_0[1+4(E-E_0)^2/\Gamma^2]^{-1} + \sigma_{\text{const}},$$

$$\sigma_0 = 4\pi\lambda\!\!\!^{-2} f(\Gamma_n/\Gamma) = \sigma_{0c} + \sigma_{0s},$$

$$\frac{\sigma_{0s}}{\sigma_{0c}} = \frac{\Gamma_n}{\Gamma_\gamma},$$

$$f = \tfrac{1}{2}\alpha[1 \pm (2i+1)^{-1}].$$

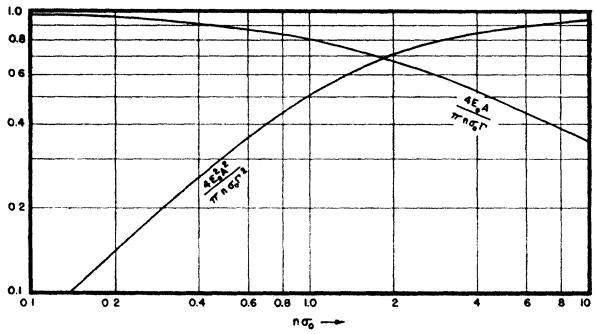

FIG. 3. The deviation of the quantities $(4E_0^2A^2/\pi n\sigma_0\Gamma^2)$ and $(4E_0A/\pi n\sigma_0\Gamma)$ from unity for intermediate values of $n\sigma_0$ are shown. Note that the area A is always smaller than should be obtained.

In the foregoing expressions σ_{const} represents that portion of the total cross section which can be considered as essentially constant in the region of resonance. $\lambda\!\!\!^{-}$ is the neutron wavelength divided by 2π and f is a statistical weighting factor for the formation of the particular compound nucleus responsible for the resonance. f is the product of the isotopic abundance, α, of the responsible isotope and the spin factor. If i is the nuclear spin of the responsible isotope, the compound nucleus can have spin $(i \pm \frac{1}{2})$ with relative statistical weights as given above. Γ_n and Γ_γ are the "neutron width" and "photon width" of the level where $\Gamma = \Gamma_n + \Gamma_\gamma$. Aside from the extra $(1/v)$ factor for capture (which is here neglected) the capture and scattering cross sections, σ_c and σ_s, show the same resonance shape. An extra interference effect[7] is expected between the potential and resonance scattering. However, this contribution to the total cross section averages to zero and is usually unimportant in our measurements. The term σ_{const} includes the total cross section near the resonance due to all other isotopes, to the other spin state, and to the potential scattering for the responsible spin state. Unless there is definite reason for using a different value, σ_{const} is usually taken as the expected value for the potential scattering for the element. If a compound is used as a sample, σ_{const} also includes the contribution from the other elements present.

For most of the resonance levels $E_0 \gg 1$ ev and Γ is less than the resolution width so the experimental curve of σ *vs* E is flattened and broadened relative to the true curve corresponding to infinitely sharp resolution. If the sample is so thin that $n\sigma_0 \ll 1$, the area of the transmission dip is proportional to $n\sigma_0\Gamma$, whereas for $n\sigma \gg 1$ it is proportional to $(n\sigma_0)^{\frac{1}{2}}\Gamma$. Thus, by comparing the areas of a transmission dip for thick and thin samples, it is sometimes possible to evaluate σ_0 and Γ separately.

Let us define a quantity A which we shall call the "relative area" of a transmission dip which is obtained as follows. The experimental transmission values, T, in the region of the dip are divided by T_{const}, due to σ_{const}, and plotted *vs* t. The area above the resultant dip in μsec/meter is divided by t_0 to give A. The analysis then gives

$$n\sigma_0\Gamma^2 = 4E_0^2A^2/\pi \text{ for } n\sigma_0 \gg 1,$$

$$n\sigma_0\Gamma = 4E_0A/\pi \text{ for } n\sigma_0 \ll 1.$$

The deviations of the quantities $(4E_0^2A^2/\pi n\sigma_0\Gamma^2)$ and $(4E_0A/\pi n\sigma_0\Gamma)$ from unity for intermediate values of $n\sigma_0$ are shown in Fig. 3 for $0.1 \leq n\sigma_0 \leq 10$. It is to be noted that the area A is smaller than expected in both cases when the limiting conditions are not satisfied. The method which has been adopted for the routine evaluation of $n\sigma_0$ when measurements have been made on both thick and thin samples is to compute $\sigma_0\Gamma^2$ from A for the thick sample and again for the thin sample, using the thick sample approximation in each case. The ratio of the values $(\sigma_0\Gamma^2)_{\text{thin}}/(\sigma_0\Gamma^2)_{\text{thick}}$ will be <1 because of the bad approximation in using the thick sample formula for the thin sample. However, by comparing the value of this ratio with the curve of Fig. 3, the value of $n\sigma_0$ for the thin sample is obtained directly and thus σ_0 and Γ are separately evaluated.

If the isotope responsible for the resonance is known, then, a is known. If $i \neq 0$ then the spin of the compound nucleus having the resonance is usually not known and only $f\Gamma_n$ can be determined from σ_0 and Γ. For medium atomic weight elements having level spacings of $\sim$10 to 1000 ev, the value of Γ_n for levels of a few ev energy is usually much smaller than Γ. Some theories predict that $\Gamma_n E_0^{-\frac{1}{2}}$ should be proportional to the level spacing (for the given compound nucleus spin state). For light elements such as Mn and Co where the level spacing is large and the resonance energy is usually greater than 100 ev, it has been found, in agreement with theory, that $\Gamma_n \gg \Gamma_\gamma$ so σ_0 depends only on E_0 and f. For such cases if it is assumed that $\Gamma_n \approx \Gamma$ and the value of f is

[7] Feshbach, Peaslee, and Weiskopf, Phys. Rev. 71, 145 (1947).

approximately known, the value of σ_0 can be computed and Γ evaluated from the value of $\sigma_0\Gamma^2$. This procedure has been used in a number of cases where it seemed justified.

In cases where only $\sigma_0\Gamma^2$ is known for a resonance in an element of medium atomic weight and $E_0 \ll 100$ ev, the values of σ_0 and Γ_n are sometimes estimated by assuming $\Gamma_n \ll \Gamma_\gamma \sim 0.1$ ev since values of Γ_γ have been measured in many cases and seem to be roughly constant at ~ 0.1 ev. In some cases where this last method is used to estimate σ_0, the value of $n\sigma_0$ for the sample may not satisfy the thick sample condition and the computed value of $\sigma_0\Gamma^2$ may be increased slightly by use of Fig. 3. In cases where the resultant calculated σ_0 is not $\gg \sigma_{\max}$ from the experimental transmission curve, the values of σ_0 and Γ for a given $\sigma_0\Gamma^2$ are adjusted to give the best fit between the predicted and experimental values of $\sigma_{\max}$, the predicted value being obtained by averaging the theoretical transmission curve over the experimental resolution function with the resolution function centered at t_0.

In presenting the results of an analysis of an experimental transmission curve, the appropriate method of those listed above is used. When a curve shows many resonance dips, only the first few can usually be expected to be due to single resonances and the structure at higher energies is due to the fluctuations in the distribution of many levels, the relative resolving power of the instrument decreases rapidly at higher energies while there is not expected to be any systematic change in the level spacing with energy. The maximum energy at which separate resonances can be distinguished is relative and may be a few ev when the level spacing is <10 ev. On the other hand single levels at a few hundreds or thousands of ev may be easily distinguished for the light elements which have very strong ($\Gamma_n \approx \Gamma \gg 1$ ev) widely spaced (>1000 ev) levels. Thus with less than 1 percent of Co or Mn impurities in other samples the Co and Mn dips are still observed.

G. RESULTS

Check of the Positions of the Main Resonances in Gold and Silver

After the development of the technique for measuring t_d using the thick paraffin filter, the positions of the main resonances in Au and Ag were checked. The results are shown in Figs. 4 and 5. The new values for the resonant energies are slightly higher than the previous results[2] and give $E_0 = (4.87 \pm 0.07)$ ev for gold and $E_0 = (5.13 \pm 0.07)$ ev for silver. This last result is in good agreement with the recent determination of Selove.[5] This and other measurements suggest that the earlier reported energy values tended to be slightly low and a uniform decrease of about 0.2 to 0.3 μsec/m in the earlier timing values is indicated as a proper correction. This shift is usually quite small, but not negligible, when precise energy values are desired.

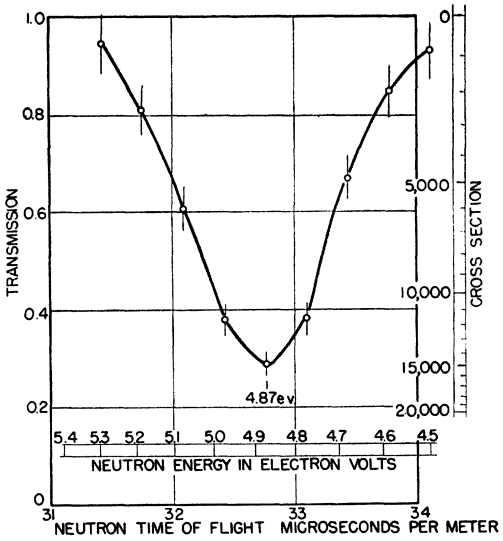

FIG. 4. The slow neutron transmission of 0.02745 g/cm² of gold.

Bromine and Sodium Bromide

Two different samples were used to study Br. The first sample contained 15.0 g/cm² powdered NaBr. The sample was of analytical reagent grade. The results of measurements with this sample are given in Fig. 6 and show sufficient structure so that it was considered of interest to prepare a sample of liquid Br. The sample was analytical reagent grade bromine dried with P_2O_5 and distilled into a quartz sample holder. Analysis showed $I < 0.05$ percent. The sample contained 16.41 g/cm² of bromine. A quartz blank containing the same amount of fused quartz as the sample holder was used as dummy on the "sample out" runs.

The measurements with liquid Br used arc and

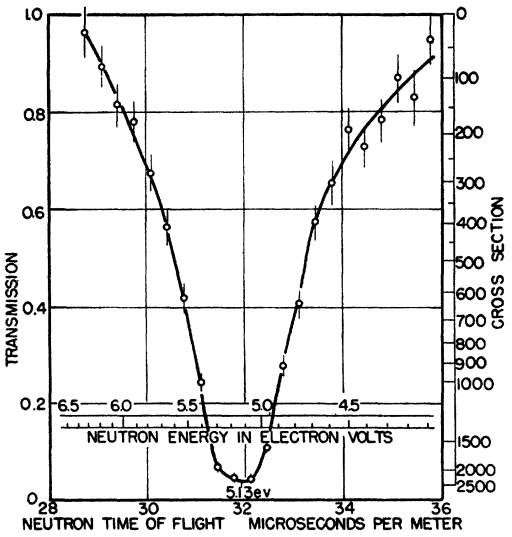

FIG. 5. The slow neutron transmission of 0.252 g/cm² of silver.

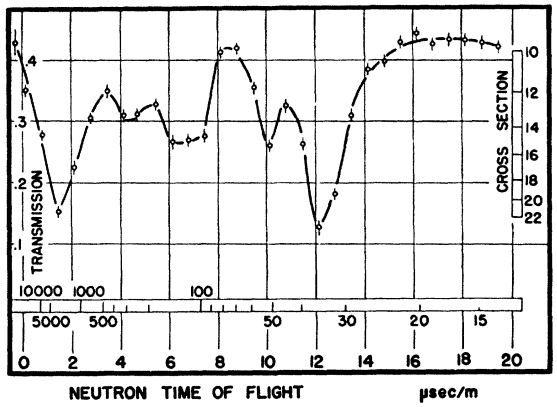

FIG. 6. The slow neutron transmission of 15 g/cm² of NaBr.

detector "on times" of $\tau_{arc}=4$ μsec and $\tau_{det}=2$ μsec for a resolution triangle base width of about 1 μsec/m. The measurements of NaBr used $\tau_{arc}=\tau_{det}=4$ μsec and extend as low as 13 ev. The two curves agree on the position of the resonance dips at 35.7 ev and 54 ev. A broad dip near 100 ev in NaBr is resolved into dips at 104 ev and 136 ev using the higher resolution for Br. Except for the strong dip near 3000 ev for NaBr, the two samples seem to agree as well as possible for the general behavior of the whole curve, but more detail is seen at higher energies in Fig. 7. The strong dip near 3000 ev clearly must be due to Na, and this has been confirmed by recent work of Selove.[5]

In Fig. 7 Br shows a dip between 4 and 5 μsec/m which is probably due to two or more levels. If two levels are responsible, they are near 260 and 320 ev. The dip near 700 ev and the broad dip at higher energies are probably due to a large number of levels since an average level spacing of less than 100 ev is indicated. Although the energy region below 13 ev is not shown in these curves, it has been measured carefully by I. W. Ruderman (private communication) in connection with other studies and shows no levels at lower energies. The cross section in the thermal region is well matched by the relation $\sigma=(5.95+1.01E^{-\frac{1}{2}})$ barns.

Natural Br contains 50.6 percent Br^{79} and 49.4 percent Br^{81} both with spin $\frac{3}{2}$. Neutron capture by Br^{79} gives Br^{80} which has two isomeric states with half-lives of 4.4 hours and 18 min decaying by electron and positron emission to Kr^{80} and Se^{80}. Neutron capture by Br^{81} gives 34-hour β-active Br^{82}. Both isotopes are known to be produced by thermal neutron capture[8] with roughly equal cross sections. Thus there are four ways in which a compound nucleus can be formed considering the two isotopes each with possible spin $I=1$ and $I=2$ with relative spin statistical weights $\frac{3}{8}$ and $\frac{5}{8}$. Since the total statistical weight factor f is either 0.19 or 0.31 in all cases, the four possibilities, for the purposes of this analysis, can be considered to have almost equal statistical weights and *a priori* chance of being responsible for any given resonance level. However, the four states may not all have levels of the same strengths or spacings. In the analysis of the level strengths only the first few levels have been considered in detail since the other dips are probably due to more than one level. For the first two levels, the analysis was also made using the NaBr curve as a check.

For the first level at 35.7 ev the Br curve gives $\sigma_0\Gamma^2=210$ barns (ev)² while the NaBr curve gives 275 barns (ev)². Since the Br curve seems better for this analysis, a weighted average of 220 barns (ev)² is used. If we assume $\Gamma_n\ll\Gamma_\gamma\approx 0.1$ ev, then $\sigma_0\approx 2.2\times 10^4$ b. If we use $f\approx 0.25$ for the responsible isotope, then $\sigma_0\approx 1.9\times 10^4\,\Gamma_n/\Gamma$ which gives $\Gamma_n\approx\Gamma$. Thus the original assumptions are not good. If we assume $\Gamma_n=\Gamma_\gamma$ then $\sigma_0\approx 9\times 10^3$ b from theory and $\Gamma=2\Gamma_\gamma=2\Gamma_n\approx 0.15$ ev. This corresponds to $\Gamma_n E_0^{-\frac{1}{2}}\approx 0.026$ (ev)$^{\frac{1}{2}}$. (Note that σ_0 always refers to the element.)

The second level at 54 ev has $\sigma_0\Gamma^2=140$ barns (ev)² from the Br curve and 100 barns (ev)² from the NaBr curve. In this case the Br curve is much more reliable and the value 140 is used. If we assume $\Gamma_n\approx\Gamma_\gamma$ and $f\approx 0.25$, then $\sigma_0=6.15\times 10^3$ b and $\Gamma\approx 0.15$ ev as for the other level. This corresponds $\Gamma_n E_0^{-\frac{1}{2}}\approx 0.021$ (ev)$^{\frac{1}{2}}$.

For the third level at 104 ev, the Br curve gives $\sigma_0\Gamma^2=250$ b (ev)². Assuming $f\approx 0.25$ and $\Gamma_n\approx 3\Gamma_\gamma$ gives $\sigma_0\approx 4700$ b and $\Gamma\approx 0.24$ ev. The larger value of Γ_n/Γ_γ is assumed to keep Γ_γ about the same as for the other levels whereas Γ_n should increase with energy. This gives $\Gamma_n\approx 0.18$ and $\Gamma_n E_0^{-\frac{1}{2}}\approx 0.018$ (ev)$^{\frac{1}{2}}$.

The fourth level at 136 ev has $\sigma_0\Gamma^2=1000$ b (ev)² which is somewhat larger than the others. Assuming $f\approx 0.25$ and $\Gamma_n\approx\Gamma_\gamma$ gives $\sigma_0\approx 4800$ b and $\Gamma\approx 0.45$ ev and $\Gamma_n E_0^{-\frac{1}{2}}\approx 0.02$ (ev)$^{\frac{1}{2}}$. If this dip were really due to two equal levels, each would have $\Gamma\approx 0.23$ ev which is closer to the values for the other levels.

In the above analysis the value $f\approx 0.25$ rather than $f=0.19$ or 0.31 was used. Thus all calculated values of Γ should be increased or decreased by about 15 percent

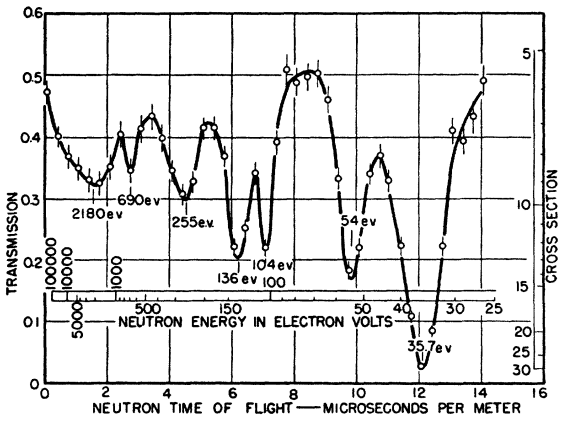

FIG. 7. The slow neutron transmission of 16.41 g/cm² of Br.

[8] National Bureau of Standards Circular 499.

depending on whether $I=1$ or 2 for the compound nucleus. Clearly the assumptions $\Gamma_n \approx \Gamma_\gamma$ are crude and this should be considered in using the resulting values of Γ_n and Γ. However, the resultant values of Γ_γ are reasonable; so the order of magnitude of the results is probably correct.

On the basis of the theory of Feshbach, Peaslee, and Weisskopf,[7] the average level spacing D should be related to $\Gamma_n E_0^{-\frac{1}{2}}$ by the approximate relation $D=5000\ E_0^{-\frac{1}{2}}\Gamma_n$. Since the values of $\Gamma_n E_0^{-\frac{1}{2}}$ are all roughly the same and equal to 0.02 (ev)$^{\frac{1}{2}}$, the predicted level spacing is about 100 ev. A further comparison with the experimental level spacing depends on whether the observed levels are all due to one of the four possible compound nucleus states or are divided among them. If the spacing of 100 ev applies separately to each state then $D=25$ ev is predicted for the element. The experimental level spacings of >35 ev (between the first level and the next at negative neutron incident energy), 18 ev, 51 ev, and 31 ev are consistent with an average spacing in this region of between 25 and 100 ev so that the agreement with theory is reasonably good. It is also of interest to note that Br is the lightest element to show such a close level spacing.

The main results for Br may be summarized as follows:

1. In the thermal region Ruderman obtained $\sigma=5.95+1.01E^{-\frac{1}{2}}$.
2. The first level has $E_0=35.7$ ev with $\sigma_0\Gamma^2=220$ b (ev)^2. If $\Gamma_n\approx\Gamma_\gamma$ then $\sigma_0\approx 9\times 10^3$ b, $\Gamma\approx 0.15$ ev and $\Gamma_n E_0^{-\frac{1}{2}}\approx 0.026$ (ev)$^{\frac{1}{2}}$.
3. The second level at 54 ev has $\sigma_0\Gamma^2=140$ b (ev)^2. If $\Gamma_n\approx\Gamma_\gamma$ then $\sigma_0\approx 6\times 10^3$ b, $\Gamma\approx 0.15$ ev and $\Gamma_n E_0^{-\frac{1}{2}}\approx 0.02$ (ev)$^{\frac{1}{2}}$.
4. The third level has $E_0=104$ ev and $\sigma_0\Gamma^2=250$ b (ev)^2. If $\Gamma_n\approx 3\Gamma_\gamma$, then $\sigma_0\approx 4700$ b, $\Gamma\approx 0.24$ ev and $\Gamma_n E_0^{-\frac{1}{2}}\approx 0.018$ (ev)$^{\frac{1}{2}}$.
5. The fourth level has $E_0=136$ ev and $\sigma_0\Gamma^2=1000$ b (ev). If it is single and $\Gamma_n\approx\Gamma_\gamma$, then $\sigma_0\approx 4800$ b, $\Gamma\approx 0.45$ ev and $\Gamma_n E_0^{-\frac{1}{2}}\approx 0.02$ (ev)$^{\frac{1}{2}}$.
6. There is evidence for many more unresolved levels at higher energies.
7. In addition, the NaBr shows a strong level in Na near 3000 ev in agreement with Selove.[5]

In conclusion we also point out that the resolving power of the instrument is well illustrated by the degree of resolution of the dips at 6.2 and 7.1 μsec/m and the sharp rise on the low energy sides of the resonance.

Iron

The slow neutron transmission of the sample of iron containing 9.93 g/cm^2 has been reinvestigated.[3] The results of the transmission measurements using broad resolution are shown in Fig. 8. Spectroscopic analysis of the sample showed between 0.5 and 1 percent Mn, 0.01 to 0.05 percent Cr, about 0.001 percent Co, between 0.01 percent and 0.1 percent Cu, and traces of Ag and

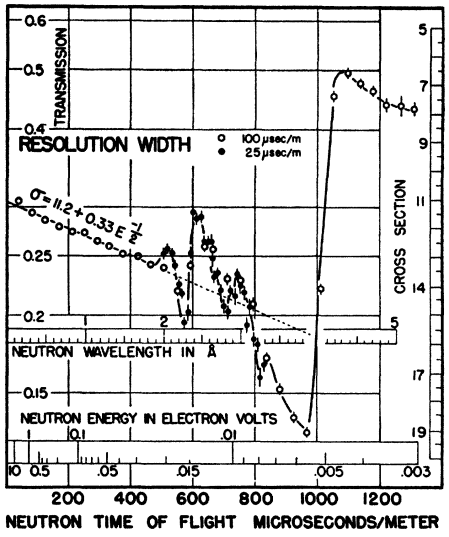

FIG. 8. The slow neutron transmission of 9.93 g/cm^2 of Fe. The sharp changes are caused by crystal interference effects.

Pb. The results in the region between 2 ev and 0.03 ev are well matched by the relationship $\sigma=(11.2+0.33E^{-\frac{1}{2}})$ barns. This is in good agreement with earlier results.[3]

Below 0.02 ev strong crystal interference effects are observed. At the suggestion of Professor O. Halpern, the wavelength interval between 2A and 3A was investigated with higher resolution than is usually used in order to resolve the discontinuities in the transmission corresponding to the Debye-Scherrer rings at 2.3A and 2.8A predicted by theory. The theory also predicts that the coherent scattering for iron should disappear at the cut-off wavelength of 4.04A. The large change in transmission between 3.8A and 4.2A indicates the close agreement obtained between observed transmission and the theoretical prediction. The agreement between theory and experiment for the passage of neutrons through polycrystalline media is very gratifying.

At 0.003 ev the predicted σ_c from the thermal slope is 6.0 b compared to the measured total cross section of 7.8 b. Thus 1.8 b is due to residual incoherent scattering.

The results of the transmission measurement above 200 ev are shown in Fig. 9. The dips near 330 and 4000 ev are caused by the manganese impurity. From the area of the dip at 330 ev the sample should contain 0.7 percent manganese which is in good agreement with the spectroscopic analysis. The dip at 950 ev cannot be attributed to any specific impurity, as none of the observed impurities have known levels at this energy. However, because of the small magnitude of the dip and the statistical uncertainty of the points involved, no conclusions have been drawn about this level. It might be due to one of the rarer isotopes of iron or to some other impurity.

The scattering cross section in this energy region is

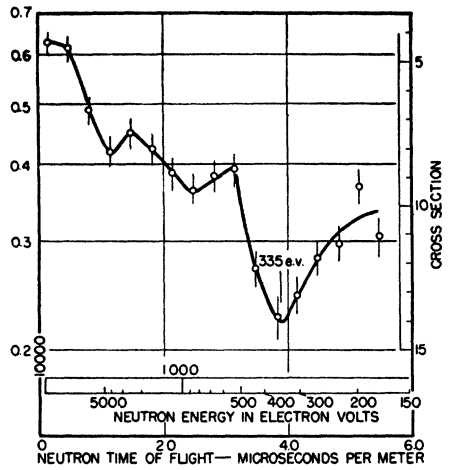

FIG. 9. The slow neutron transmission of 9.93 g/cm² Fe in the higher energy region. The dips in transmission are probably due to impurities in the iron.

much higher than $4\pi R^2$ (5.5 barns) which would indicate that there is interference between potential and resonance scattering. Because of the presence of these impurities it is difficult to determine how the scattering cross section decreases with energy in this region in order to observe the detailed behavior of the interference. Barshall *et al.*[9] found many levels in Fe below 1 Mev with the lowest at 15 kev.

Cobalt

The behavior of the Co cross section above 70 ev was reinvestigated with maximum resolution using the same 1.06 g/cm² sample which was previously studied.[2] Results of these measurements are shown in Fig. 10.

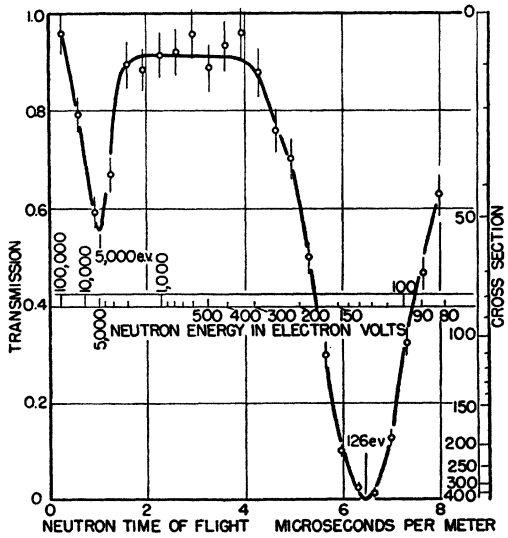

FIG. 10. The slow neutron transmission of 1.06 g/cm² of Co showing the resonances at 126 and 5000 ev.

[9] Barschall, Bockelman, and Seagondollar, Phys. Rev. **73**, 659 (1948).

A spectroscopic analysis of the sample showed about 1 percent Ni, 0.05 percent Mn, less than 0.01 percent Zn and Cr, and traces of Al, Ca, Cu, Fe, Mg, Si, and Na. The results for the cross section at lower energies are given in the earlier paper.[2]

The earlier measurements showed a strong dip at 115 ev which is now placed at 126 ev in line with the above remarks. The curve shows the main resonance dip at 126 ev and a higher energy dip near 5000 ev. The higher energy dip may be due to several levels. It is unlikely that an impurity could give such a strong dip so it is probably due to Co.

The level at 126 ev must be the result of the main (99.83 percent) Co^{59} isotope of spin 7/2. It has also been studied in detail by Seidl[10] using Co as a resonance scattering detector. Seidl has shown that this level has $\Gamma_n \gg \Gamma_\gamma$ and obtains $\Gamma = 2.0 \pm 0.1$ ev if $I=4$ for the compound nucleus and $\Gamma = 5.0 \pm 0.5$ ev if $I=3$. His measured value of $\sigma_0 = 12{,}500 \pm 1250$ b is consistent

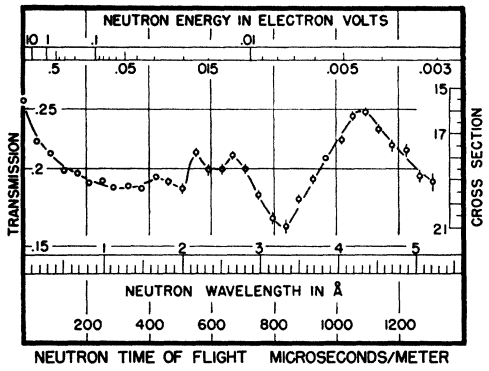

FIG. 11. The slow neutron transmission of 8.47 g/cm² of Ni. The abrupt changes in transmission are caused by crystal interference effects.

only with $I=4$. For 126 ev the predicted values of σ_0 for $\Gamma_n \gg \Gamma_\gamma$ are 9100 b for $I=3$ and 11,600 b for $I=4$.

Analysis of the area of the dip at 126 ev in Fig. 10 gives $\sigma_0 \Gamma^2 = 2.3 \times 10^5$ b (ev)² which gives

$$\Gamma = 5.0 \text{ ev for } I=3, \quad \Gamma = 4.4 \text{ ev for } I=4.$$

These results for Γ, when combined with those of Seidl, argue strongly for $I=3$ in disagreement with his conclusion.

In conclusion, the analysis of the dip at 126 ev, when combined with Seidl's results, favors $I=3$, $\sigma_0 \Gamma^2 = 2.3 \times 10^5$ b (ev)², $\sigma_0 = 9100$ b, $\Gamma_\gamma \ll \Gamma_n \approx 5.0$ ev, and $\Gamma_n E_0^{-\frac{1}{2}} = 0.45$ (ev)$^{\frac{1}{2}}$. Analysis of the dip at 5000 ev, assuming that it is a single level, gives $\sigma_0 \Gamma^2 \sim 2 \times 10^8$ b (ev) or $\Gamma \sim 900$ ev, which seems unreasonably large. Therefore, probably more than one level is responsible for this dip.

Nickel

The slow neutron transmission of Ni was remeasured using the same samples as in the earlier studies.[3] Spec-

[10] F. P. G. Seidl, Phys. Rev. **75**, 1508 (1949).

trographic analysis of the sample showed 0.9 percent Co, 0.3 percent Mn, 0.02 percent Cr, between 0.1 and 0.9 percent Fe, Hg, and Si, between 0.01 percent and 0.09 percent Al, B, Cu, Ti, and between 0.001 and 0.009 percent Ca, Mg. The measurements in the thermal region were extended to 0.003 ev and the results are shown in Fig. 11. The curve shows strong interference effects over most of the wavelength region.

The earlier measurements[3] had shown a resonance dip near 100 ev and so the region above 90 ev was reinvestigated using highest resolution and the results are shown in Fig. 12. The dips near 130 ev and 330 ev are believed to be due to cobalt and manganese, respectively. From the area of the dip near 130 ev it is calculated that the sample contains 0.85 percent cobalt, which is in good agreement with the result of 0.9 percent obtained for this sample by spectroscopic analysis.

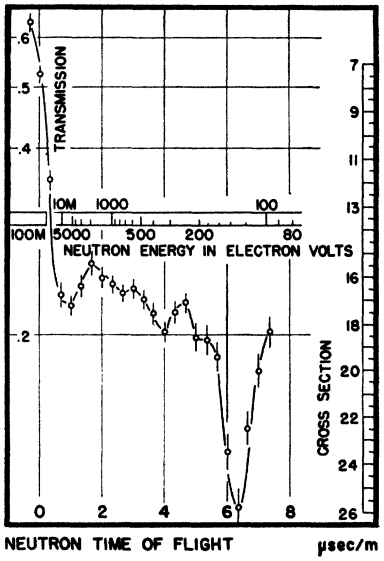

FIG. 12. The slow neutron transmission of 8.47 g/cm² of Ni in the higher energy region. The dip near 130 ev is due to a Co impurity and the other dips are probably due to other impurities.

From the area of the dip at 330 ev the Mn impurity was calculated to be between 0.2 percent and 0.8 percent in agreement with the spectroscopic analysis of 0.3 percent. The dip at 5000 ev probably represents a resonance in one of the nickel isotopes. However, this conclusion is somewhat uncertain as it could be caused by levels in impurities such as Cr, Mn, and Co. An attempt to explain this dip on the basis of any of these elements would require larger amounts of these materials than found from the spectroscopic analysis.

The results for Ni are similar to those for Fe in that the scattering cross section remains relatively constant at ~3 to 4 times the value expected for potential scattering over a wide energy region. The presence of the impurity resonances makes it difficult to observe the details of the decrease in cross section above 1000 ev to give a prediction of the expected level density according

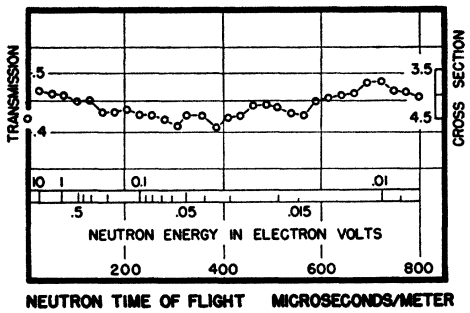

FIG. 13. The slow neutron transmission of 20.93 g/cm² of Zn in the low energy region. The changes in transmission shown are caused by crystal interference effects.

to the theory of Feshbach, Peaslee, and Weisskopf.[7] The results of Barshall *et al.*[9] show many resonances below 1 Mev.

Zinc

The slow neutron transmission of two samples of zinc containing 20.93 g/cm² and 42.29 g/cm² were investigated. The samples were made by casting the analytical reagent grade zinc in a carbon crucible. Spectrographic analysis of the sample showed Mn and Cr to be present to less than 0.01 percent and traces of B, Si, Fe, Sr, Mg, Pb, Cu, Ag, and possibly Cd.

The results of the transmission measurements using broad resolution on the 20.93 g/cm² sample are given in Fig. 13. The results in the region between 2 ev and 0.06 ev are well matched by the relation,

$$\sigma = (3.86 + 0.17E^{-\frac{1}{2}}) \text{ barns.}$$

The irregularities in the transmission at large times-of-flight are caused by neutron interference effects due to the crystalline structure of the sample.

The energy region above 0.5 ev was studied using high resolution with the results shown in Fig. 14. Below 100 ev the curve agrees well with the straight line determined from the data in Fig. 13. Above 100 ev there are very definite dips in transmission which indicate one or more resonances at higher energies.

The region above 200 ev then was investigated using

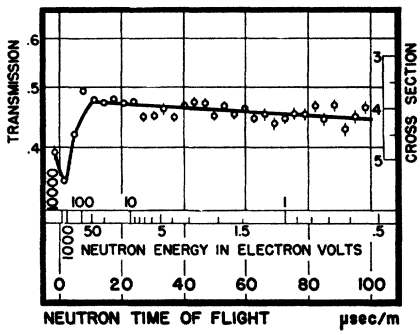

FIG. 14. The slow neutron transmission of 20.93 g/cm² of Zn in the intermediate energy region showing the $1/v$ line $\sigma = (3.86 + 0.17E^{-\frac{1}{2}})$ and the resonances at higher energy.

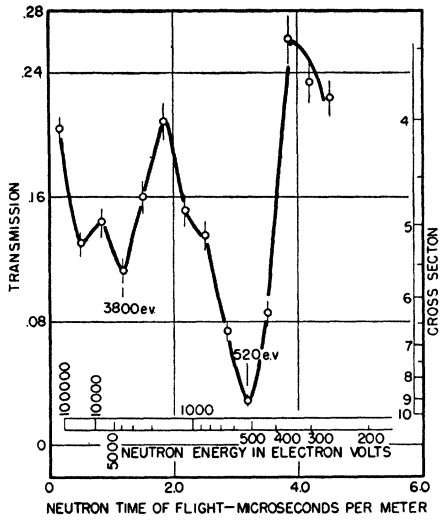

FIG. 15. The slow neutron transmission of 42.29 g/cm² of Zn in the higher energy region.

maximum resolution on the 42.29 g/cm² sample. The results are shown in Fig. 15. The curve shows a strong resonance at 520 ev, a probable partially resolved level near 1100 ev, a dip at 3800 ev, and a dip probably due to many levels above 15,000 ev. Since zinc has about the same atomic weight as Mn, Cr, and Co, therefore the levels would be expected to be strong, widely spaced, and principally due to scattering. The first two or three dips are probably caused by single levels and have been analyzed as such. The dip in transmission above 10,000 ev is probably caused by more than one level; therefore no analysis has been made.

Natural zinc has 5 isotopes: 50.9 percent Zn^{64}, 27.3 percent Zn^{66}, 17.4 percent Zn^{68}, 3.9 percent Zn^{67}, and 0.5 percent Zn^{70}. Four of these isotopes are of the even-even type and probably have spin zero and therefore the f is determined by the isotopic abundance. Zn^{67} has a spin 5/2; therefore the total statistical weight factor would be 0.016 or 0.024, depending on the spin of the compound nucleus.

There are two activities known to be produced by slow neutron reaction in zinc. These are the 57-min period[8] produced by $Zn^{68}(n,\gamma)Zn^{69}$ and a 210-day period[8] produced by $Zn^{64}(n,\gamma)Zn^{65}$. Two other activities[8] produced by neutrons are the 5-min $Zn^{66}(n,p)Cu^{66}$ and 12.5-hr $Zn^{64}(n,p)Cu^{64}$.

TABLE I.

A	64	66	67	68	70
f	0.509	0.273	0.024 0.016	0.174	0.005
Γ(ev)	5.2	7.1	24 29	8.9	52
$\Gamma_n E^{-\frac{1}{2}}$	0.23	0.31	1.3 1.1	0.40	2.3

TABLE II.

A	64	66	67	68	70
Γ	4.4	6.0	20 25	7.6	45
$\Gamma_n E_0^{-\frac{1}{2}}$	0.13	0.18	0.61 0.75	0.23	1.4

The dip in transmission with a minimum at 520 ev does not recover fast enough on the high energy side of the resonance and seems to be caused by two levels, one at 520 ev and the other at 1100 ev. Since the levels have not been completely resolved, the curve was divided into two separate dips by comparing this transmission curve with those of elements having single resonances in this energy region. The area of the dip at 520 ev corresponds to $\sigma_0\Gamma^2=6.9\times10^4$ barns (ev)². Assuming $\Gamma_n\gg\Gamma_\gamma$ gives $\sigma_0=5100\,f$ barns and $\Gamma=3.7\,f^{-\frac{1}{2}}$ ev where f is the total statistical factor. The results for this level for the different isotopes are given in Table I. The values of $\Gamma_n E^{-\frac{1}{2}}$ are so large for Zn^{67} and Zn^{70} that it seems unlikely that this level can be attributed to these rare isotopes.

The second dip at about 1100 ev is much more uncertain both in the determination of the energy of the resonance and the area of the resonance. The area had to be determined from a relatively small fraction of the total dip caused by the two unresolved levels. The result obtained for this level is $\sigma_0\Gamma^2=2.3\times10^4$ barns (ev)². Again assuming $\Gamma_n\gg\Gamma_\gamma$ gives $\sigma_0=2300\,f$ barns and $\Gamma=3.2\,f^{-\frac{1}{2}}$ ev. The results for the different isotopes for this level are given in Table II.

The third level at 3800 ev has been separated from the levels at higher energy in a manner similar to that which was used to separate the levels at 520 ev and 1100 ev. The results obtained for this level (see Table III), assuming $\Gamma_n\gg\Gamma_\gamma$ and $\sigma_0\Gamma^2=2.5\times10^6$ barns (ev)², $\sigma_0=700\,f$ and $\Gamma=60\,f^{-\frac{1}{2}}$. The large values of Γ and $\Gamma_n E^{-\frac{1}{2}}$ compared to those obtained for the other two levels strongly suggest that this dip is caused by more than one level.

The results for zinc give good indication of the resoving power of the system as the resolution triangle was about 1 μsec/meter at the base, but the average spacing of the detectable dips is less than 1 μsec/meter.

The level spacing of Zn on the basis of the theory of Feshbach, Peaslee, and Weisskopf would be between

TABLE III.

A	64	66	67	68	70
Γ	84	115	390 475	144	850
$\Gamma_n E^{-\frac{1}{2}}$	1.4	1.9	6.5 7.8	2.4	14

1000 and 10,000 ev for $\Gamma_n E^{-\frac{1}{2}}$ between 0.2 and 2. This is in rough agreement with the experimental results for the level spacing since this is the level spacing per isotope, for a given spin state.

We wish to thank Miss Miriam Levin who assisted with the numerous calculations involved in this paper and the members of the cyclotron staff who aided with these measurements. Thanks are also due to the United States Atomic Energy Commission for its support of this research.

PHYSICAL REVIEW VOLUME 83, NUMBER 6 SEPTEMBER 15, 1951

The Reaction $C^{14}(p,n)N^{14}$: Excited States in N^{15}

W. D. ROSEBOROUGH, J. J. G. MCCUE, W. M. PRESTON, AND C. GOODMAN
*Laboratory for Nuclear Science and Engineering, Massachusetts Institute of Technology, Cambridge, Massachusetts**

(Received June 7, 1951)

The relative neutron yield from $C^{14}(p,n)N^{14}$ has been measured for proton energies of 1100 to 2600 kev. Resonances occur at nine proton energies: 1165, 1310, 1664, 1789, 1883, 2024, 2079, 2272, and 2451 kev. The form of the yield curve and the calculated energies of the resonance levels in N^{15} are in good agreement with the results of others on the inverse reaction, $N^{14}(n,p)C^{14}$.

I. INTRODUCTION

THE excited states of N^{15} have been studied extensively.[1] As indicated schematically in Fig. 1, the virtual levels in the region of excitation somewhat above the neutron binding energy can be excited by three bombardments: $B^{11}+\alpha$, $N^{14}+n$, and $C^{14}+p$. We are concerned here with two reactions which are inverse to each other: $N^{14}(n,p)C^{14}$ and $C^{14}(p,n)N^{14}$. Both (n,p) and (p,n) reactions on stable, light nuclei lead to residual nuclei which are unstable. The recent availability of radioactive C^{14} in reasonable concentration has made this the first case in which both reactions, leading to the same compound nucleus, can be investigated.

It is expected that the yield curve, number of protons *vs* neutron energy E_n from $N^{14}(n,p)C^{14}$, should be very similar to the yield of neutrons *vs* proton energy E_p from $C^{14}(p,n)N^{14}$. The same resonances should be observed, with identical half-widths, but at higher bombarding energies, in the (p,n) reaction, by an amount equal to the (p,n) threshold energy (see Fig. 1). The cross sections are related by the principle of detailed balance.[2]

The absolute cross section $\sigma_{n,p}$ for $N^{14}(n,p)C^{14}$ has been measured by Johnson and Barschall[3] with fairly good resolution. They found three strong resonances and indications of several weaker ones in the neutron energy range 0.2 to 2.0 Mev. The neutron yield from $C^{14}(p,n)N^{14}$ was investigated by Shoupp, Jennings, and Sun.[4] Three large peaks in the neutron yield were found at energies which correlate with the later results of Johnson and Barschall. Although they used a thin target (estimated thickness 3 kev at $E_p=1.14$ Mev), their beam energy control did not suffice to resolve weaker resonances, and a detailed comparison is not possible. Because of the general interest of the reaction and its connection with parallel work in this laboratory on the total neutron cross section of N^{14}, we decided to remeasure the $C^{14}(p,n)$ yield with the good energy resolution available with the Rockefeller electrostatic generator.[5]

II. EXPERIMENTAL METHOD

Barium carbonate was obtained from Oak Ridge National Laboratory with carbon enriched to about 1.6 percent of C^{14}. This was converted to HCN and then to NaCN in a solution of NaOH.[6] The final material

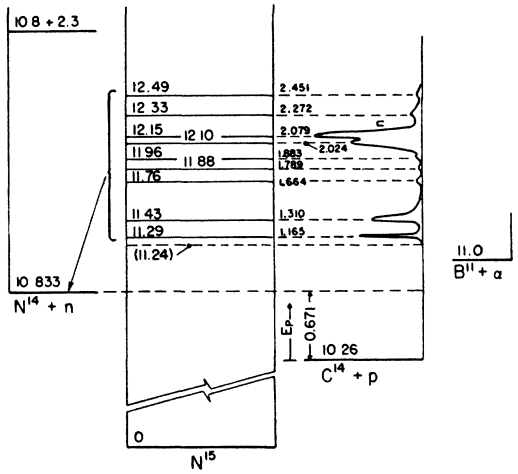

FIG. 1. Energy level diagram for N^{15} in the region somewhat above the neutron binding energy. The energies shown are computed from the results of this paper. *Note added in proof:* The energy of $C^{14}+p$ should read 10.207.

* This work was assisted by the BuShips and ONR.

[1] For a summary, see Hornyak, Lauritsen, Morrison, and Fowler, Revs. Modern Phys. **22**, 291 (1950).

[2] H. A. Bethe, *Elementary Nuclear Theory* (John Wiley and Sons, Inc., New York, 1947).

[3] C. H. Johnson and H. H. Barschall, Phys. Rev. **80**, 818 (1950).

[4] Shoupp, Jennings, and Sun, Phys. Rev. **75**, 1 (1949).

[5] W. M. Preston and C. Goodman, Phys. Rev. **82**, 316 (1951).

[6] The chemical conversion was performed by Tracerlab, Inc., Cambridge, Massachusetts.